

Positron Annihilation Spectroscopy: an Emerging Technique For Characterization of Oxygen Vacancies in Hf-based-high-k Materials?

M. Alemany^{1,4,3}, P. Desgardin⁴, A. Chabli², F. Bertin³, M. Gros-Jean¹, M.-F. Barthe⁴
¹ STMicroelectronics, 850 rue Jean Monnet, 38926 Crolles, France. ² Univ. Grenoble Alpes, INES, F-73375 Le Bourget du Lac, France. ³ CEA, LITEN, Department of Solar Technologies, F-73375 Le Bourget du Lac, France. ⁴ CNRS, CEMHTI UPR3079, Univ. Orléans, F-45071 Orléans, France.

Introduction

- High-k Metal gate (HKMG) stacks required to tackle the technological issues brought by the drastic reduction of gate length of CMOS devices (nodes < 32 nm). Use of High-k dielectrics (HfO₂) and metal gate (TiN) induces shifts in transistor V_t^{1,2} assumed to be related to oxygen vacancies (V_o) in both HfO₂ and SiO₂.³
- Charged V_o might be created during activation spike annealing giving rise to dipoles^{1,4,5} at the high-k/metal interface and thus to Fermi level Pinning⁴ which explains the V_t shift. Also, V_t shift is expected to be enhanced by oxygen vacancy creation in SiO₂ interfacial layer.^{6,7}
- To assess these mechanisms → characterization of V_o by two techniques
 - Positron annihilation spectroscopy (PAS): the most sensitive characterization method to vacancies⁸
 - Electron energy loss spectroscopy (EELS): potentially sensitive to V_o, spatial resolution compatible with HKMG structures.⁹
- PAS used to characterize vacancies in diverse materials^{10,11,12,14} but only few studies for high-k.^{8,13,15}

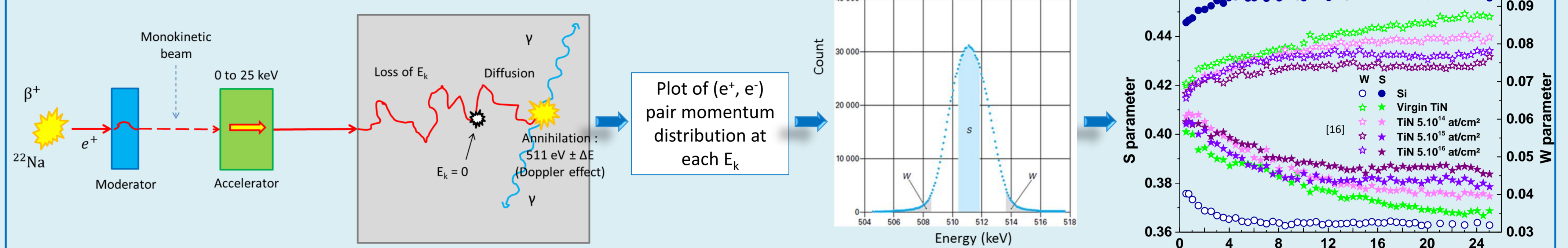
Experimental

Samples elaboration

Thickness (nm)	Deposition method	annealing
500	E-Beam – PVD	no Spike
100 – 50 – 25	Plasma sput. – PVD	no Spike
50 – 25	ALD	no Spike

- Substrates : p-type 100-oriented Si (B doped at ≈ 10¹⁵ cm⁻³)
- E-beam PVD at 150°C from an HfO₂ target
- Plasma sputtering of Hf target under Ar/O₂ atmosphere at 300°C
- Atomic Layer Deposition (ALD) at 300°C, using HfCl₄ and H₂O precursors
- Spike annealing under low N₂ pressure at 900°C during 10 s

PAS - Doppler Broadening Spectroscopy (DBS)



- Positron emission: β⁺ radioactive source ²²Na
- Moderator (monokinetic beam converter): 5 μm thick tungsten foil
- Accelerator: Kinetic energy 0.2 to 25 keV
- Flux: ≈ 10⁵ cm⁻² s⁻¹
- Detector: high purity Ge, resolution <1.14keV at 511 keV, efficiency >25% at 1.33 MeV
- Measurement of (e⁺, e⁻) pair momentum distribution by recording the Doppler broadening of the 511 keV annihilation line (ΔE)
- Extraction of low S and high W momentum annihilation fraction in respectively the momentum windows (0–|2.80|×10⁻³m₀c) and (|10.61|–|26.35| ×10⁻³m₀c) where m₀ is the mass of the electron and c, the speed of light
- S → annihilations with low momentum electrons, **valence electrons**
- W → annihilations with high momentum electrons, **core electrons**
- S and W extracted at energies ranging from 0.2 to 25 keV with step increasing from 0.2 to 1 keV

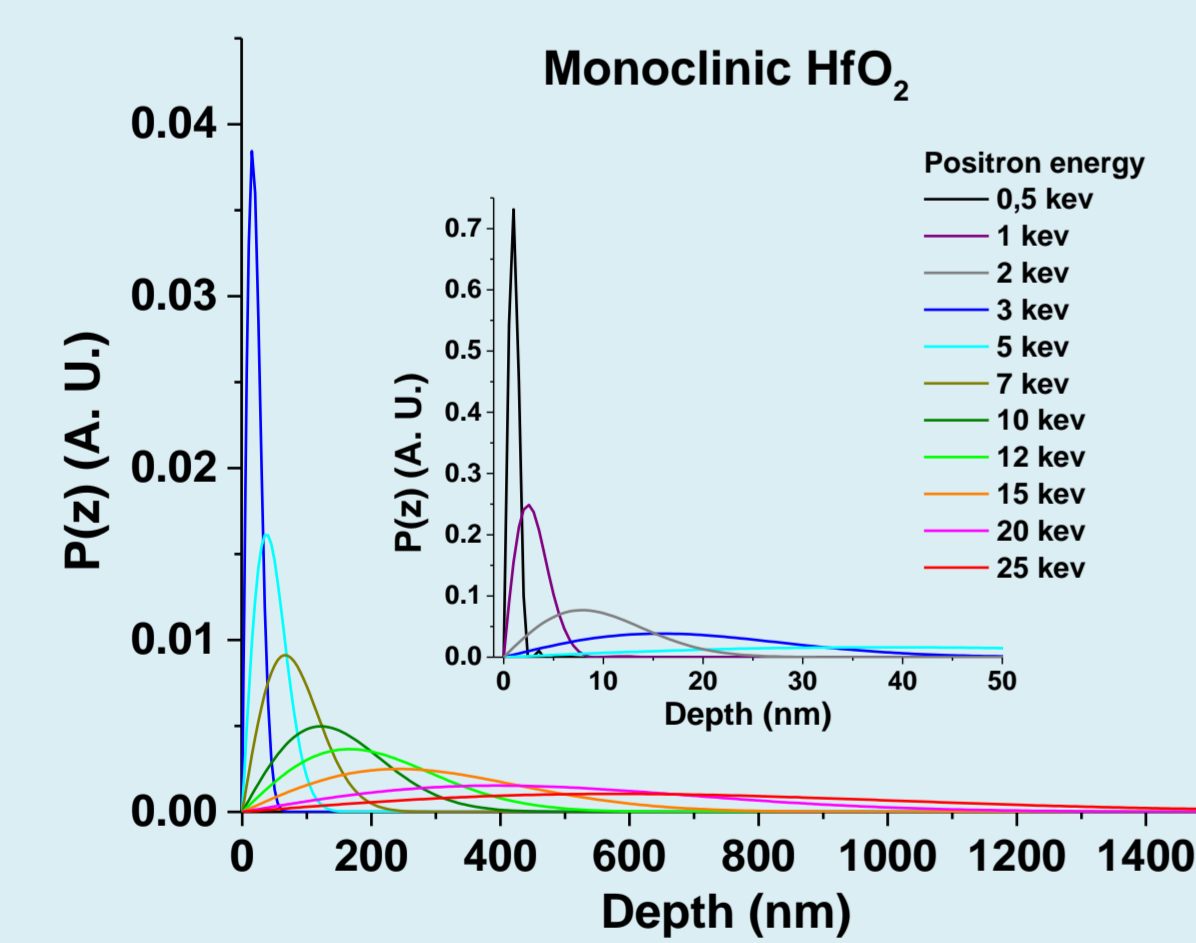
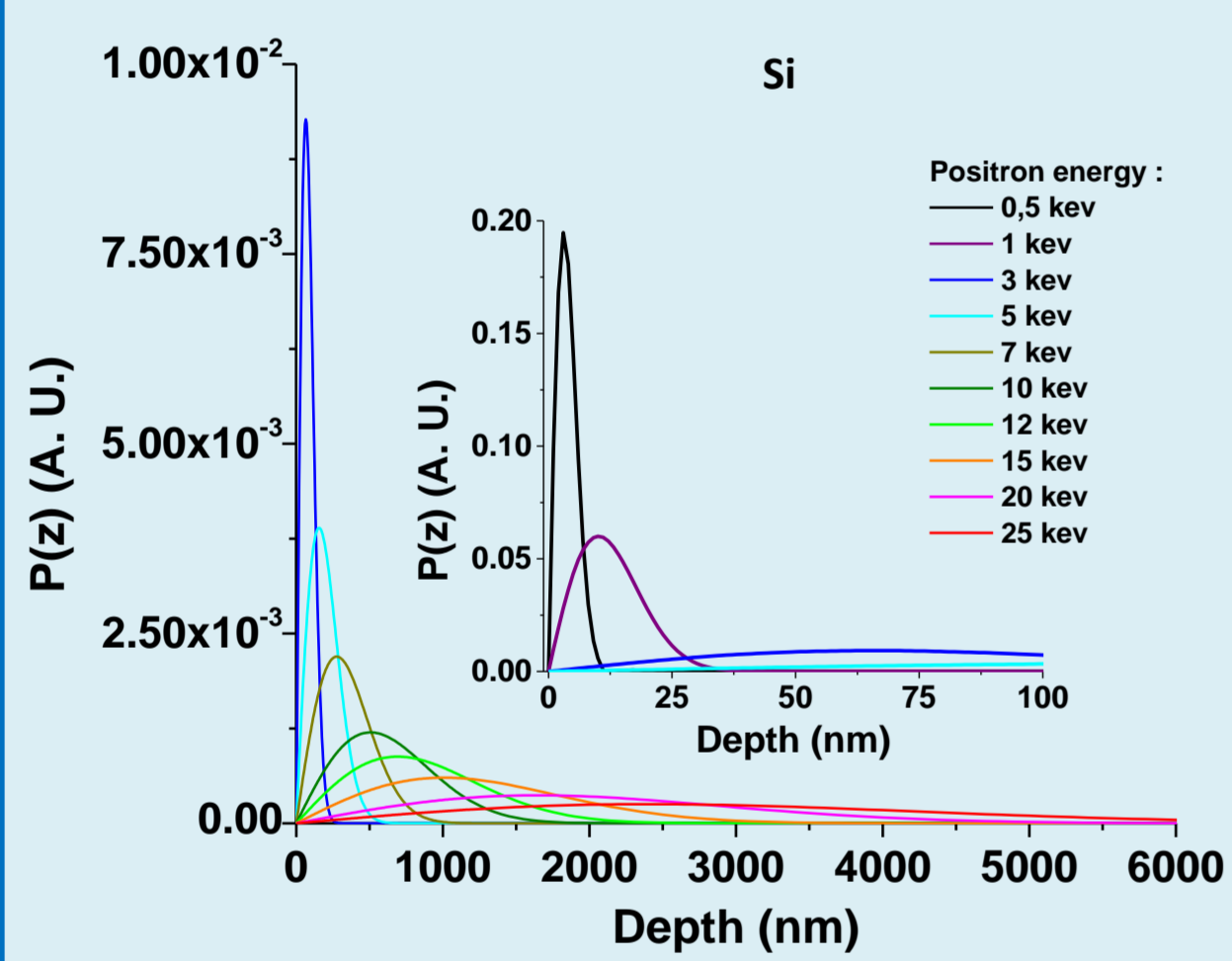
Results and discussion

PAS - Implantation profile

P(z): probability of positron implantation for each energy.
 Mean depth implantation: z_m = 0.886z₀

$$P(z) = -\frac{d}{dz} \left(e^{-\left(\frac{z}{z_0}\right)^m} \right) \quad z_0 = \frac{1}{0.886\rho} E^n$$

E: Positron energy
 ρ: material density
 A, m and n: weakly material dependent constants (p. 33 in ref. 12)

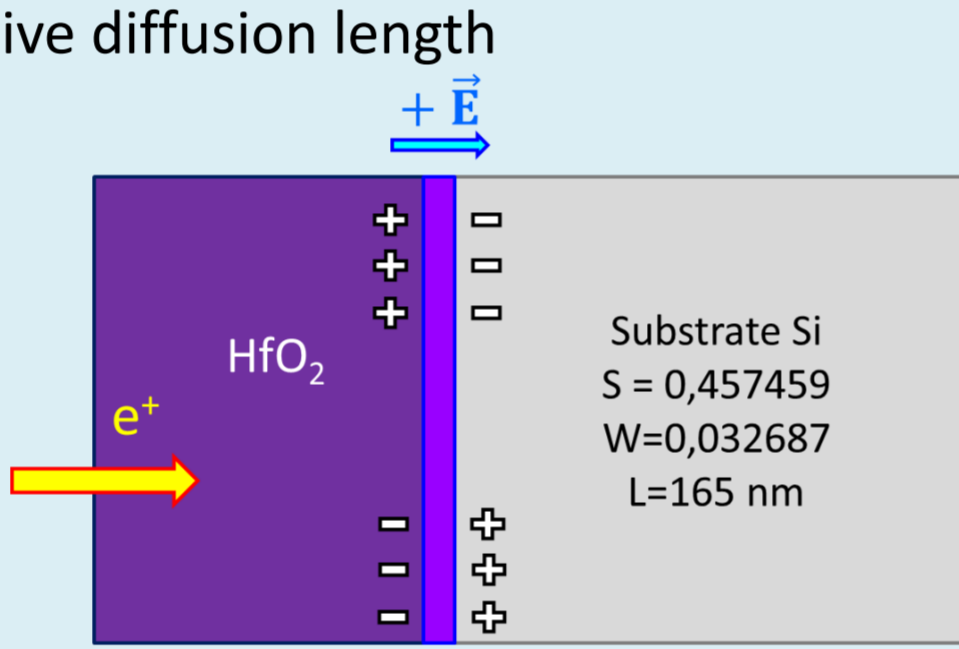


- 0.2 to 25 keV:
 - Depth interaction ≈ 8 μm in bulk silicon
 - Depth interaction ≈ 2.5 μm in HfO₂
- Below 1 keV: positron annihilation at the sample surface is predominant
- Energy range implantation For HfO₂
 - 500 nm ≈ 1 to 10 keV
 - 100 nm ≈ 1 to 5 keV
 - 50 nm ≈ 1 to 3 keV

PAS - VEPFIT simulation

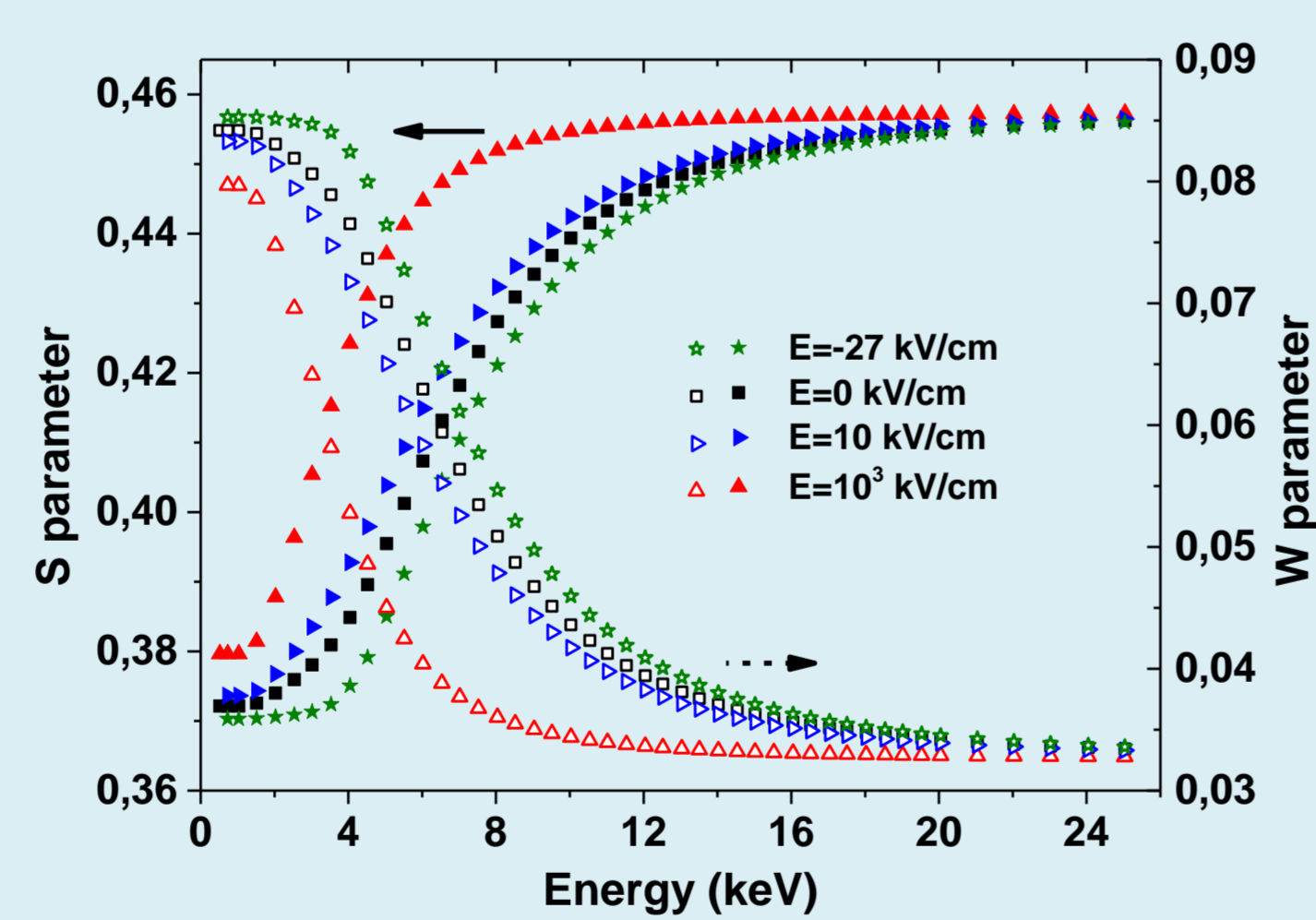
VEPFIT, fit and medialization software for PAS:

- Taking account of implantation profile and diffusion
- Sample divided into several homogenous layers
- S, W parameters determined in each layer and added, after taking account of implantation probability, to give the total S and W
- Determination of other parameters such as effective diffusion length



Simulation scheme

- 50 nm thick HfO₂ layer on Si
- Measured annihilation parameters for Si substrate, with L the diffusion length.
- Interfacial layer with electric field ranging from -27 to 10³ keV/cm

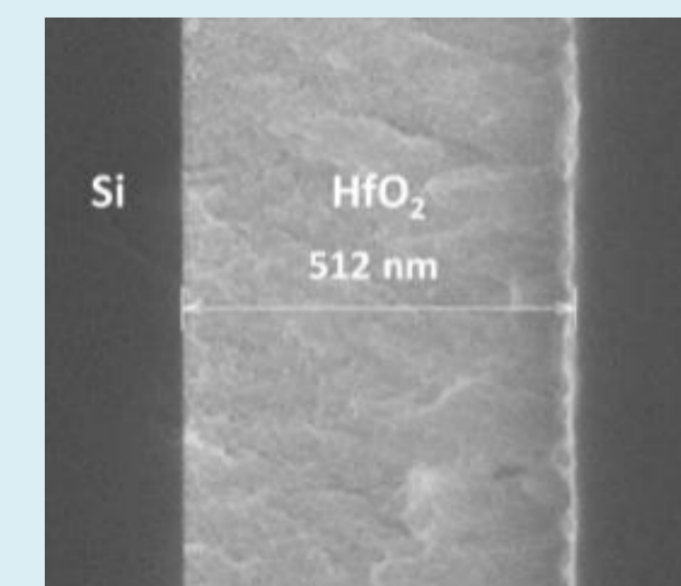
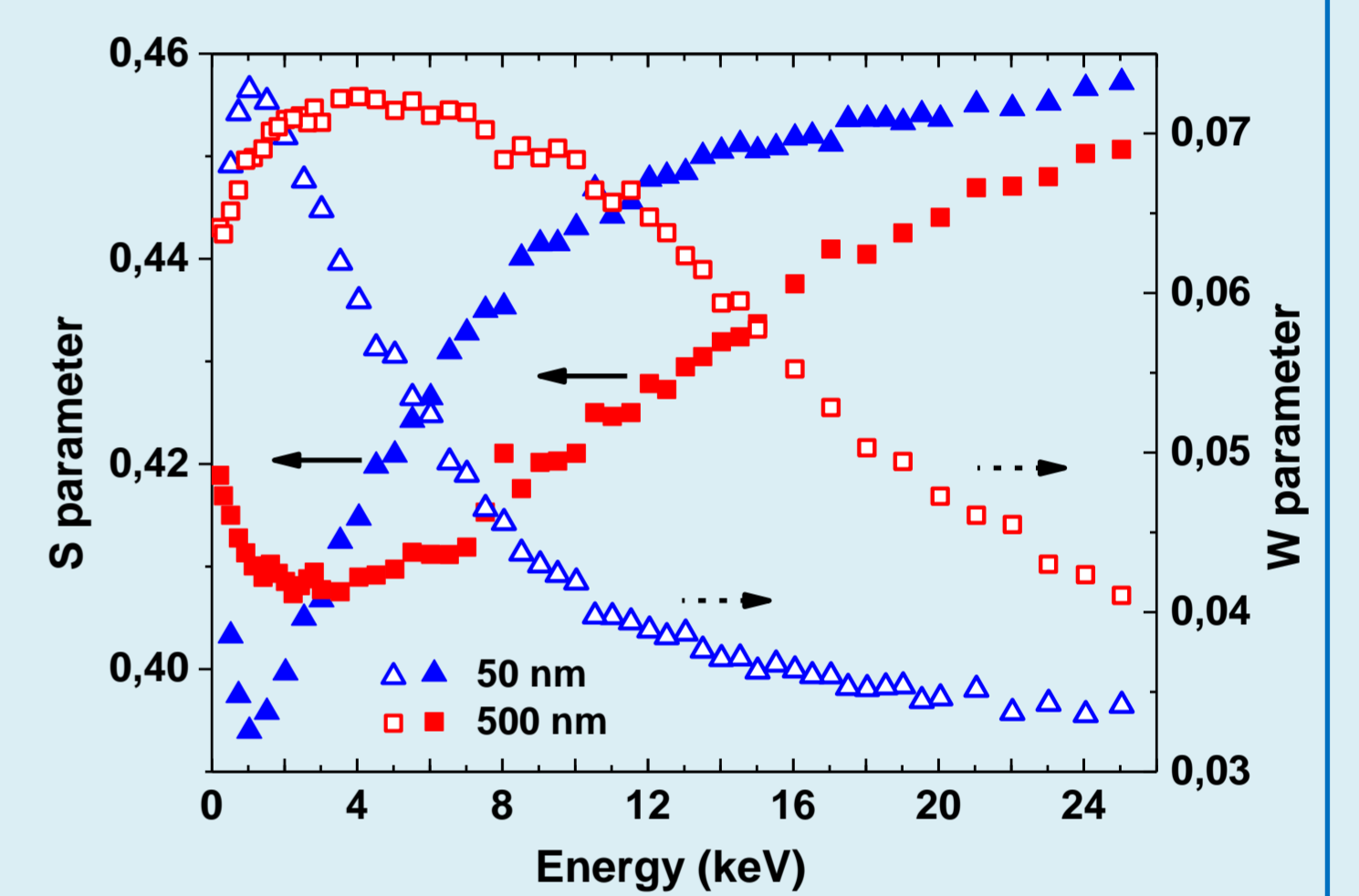


- E > 0: curves shifted towards lower energies → narrowing of the energy range governed by the HfO₂ layer → Positively charged defects at the HfO₂/Si interface.
- E < 0: curves shifted towards higher energies → broadening of the energy range governed by the HfO₂ layer → Negatively charged defects at the HfO₂/Si interface.

PAS - Results

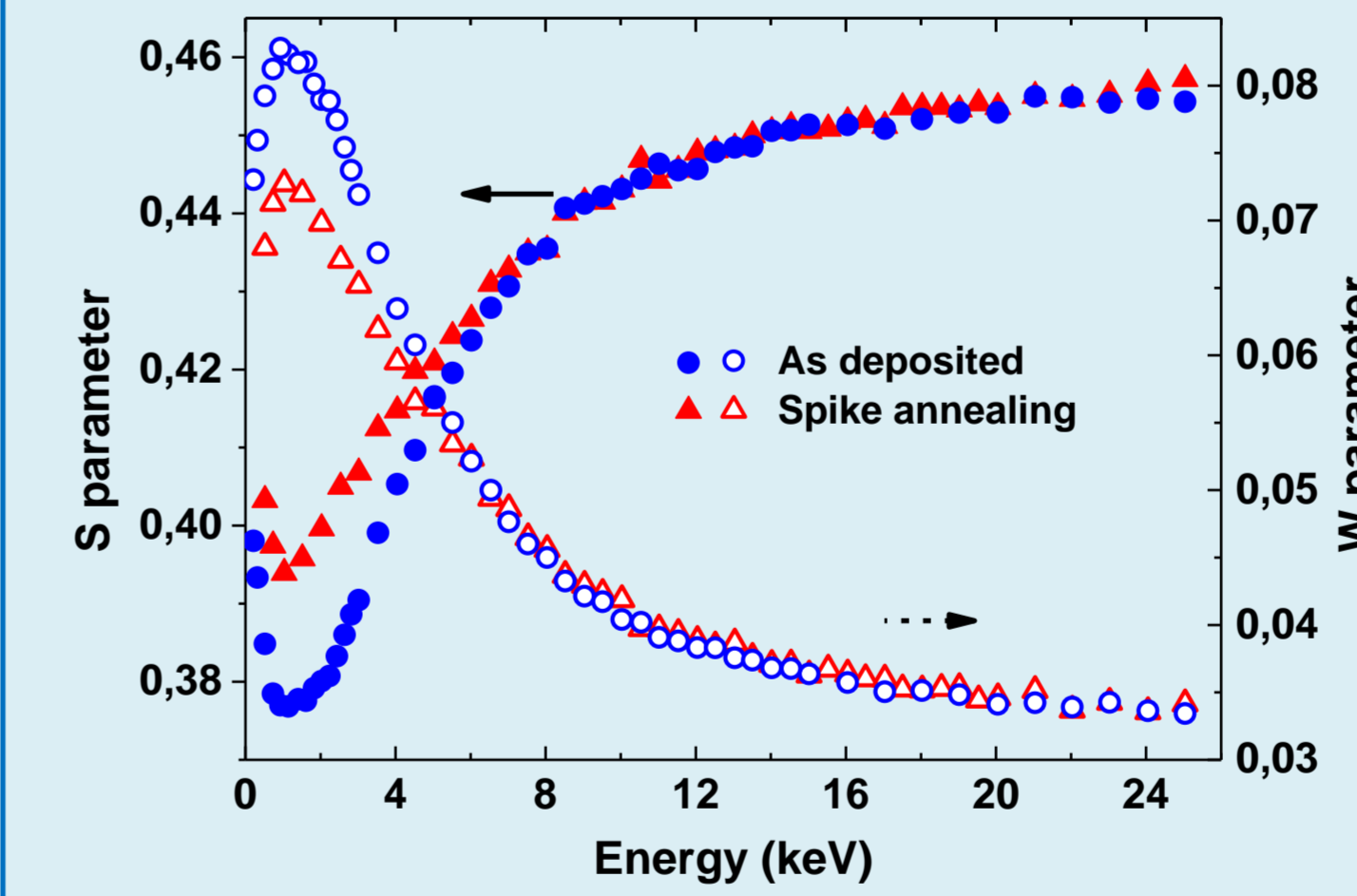
50 nm vs 500 nm (PVD, After spike annealing)

- For e⁺ beam energy > 1.5 keV (50 nm thick layer) or 6 keV (500 nm thick layer), S and W tend towards annihilation characteristics of Si → increasing annihilation fraction in substrate as the e⁺ beam increases¹⁷
- 500 nm thick HfO₂: S and W governed by annihilation in HfO₂ in the 1.5-6 keV energy range → consistent with implantation profile calculations
- 50 nm thick HfO₂: no energy range with quasi steady S and W values corresponding to HfO₂ as expected from implantation profile simulation. But S and W reach Si bulk parameters earlier → diffusion of positrons toward Si and/or a built-in electric field in the sample
- For e⁺ beam energy < 1.5 keV (50 nm thick layer) or 3 keV (500 nm thick layer): S and W governed by surface characteristics.
- S ↑ for the large HfO₂ layer → large concentration of defects suggested. Consistent with cross section SEM → 500 nm thick film very heterogeneous.



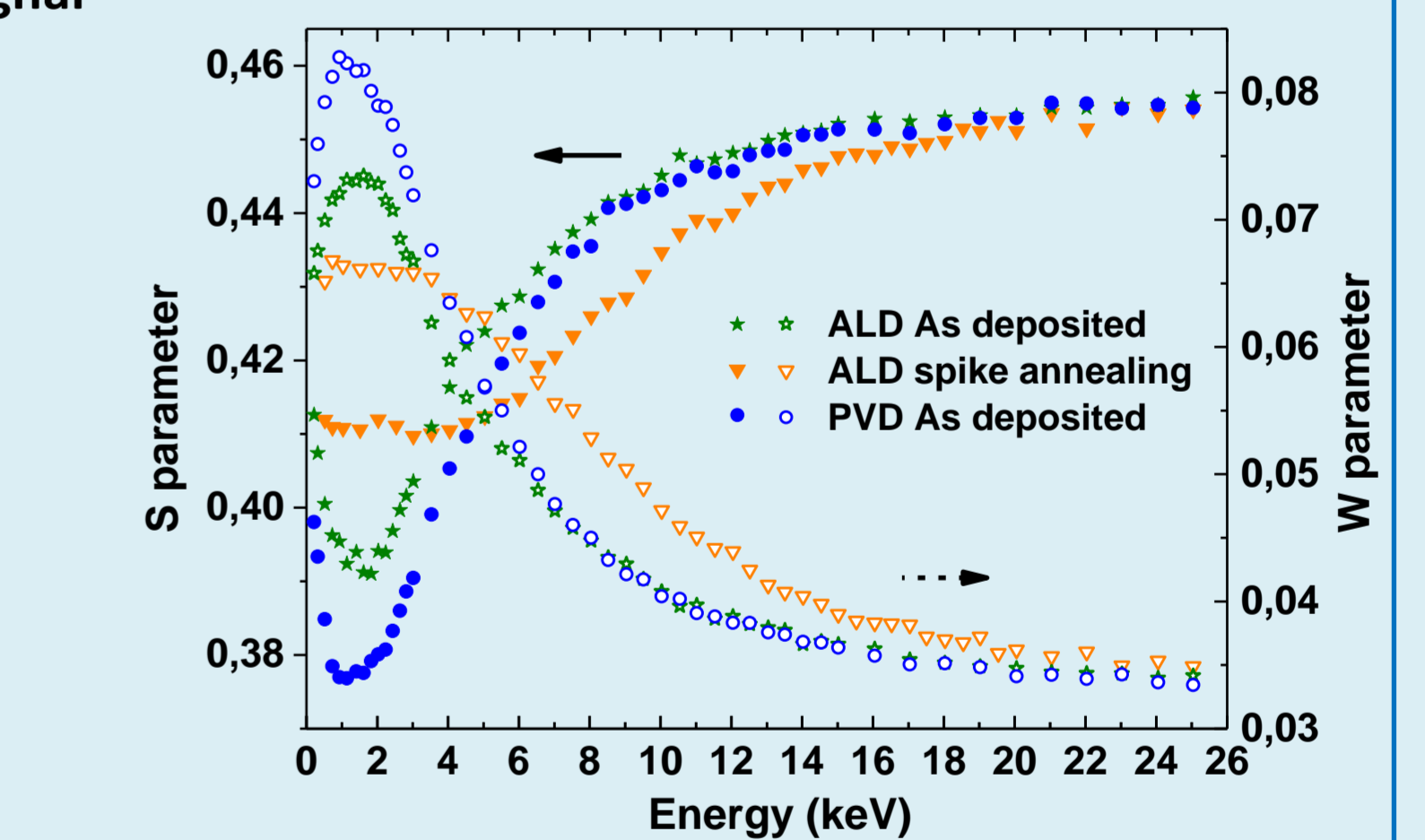
SEM observation of PVD layer of HfO₂ on Si

- Ultra-thin HfO₂ layers more difficult to analyze using PAS. Need for thick layers to minimize substrate PAS signal and to establish intrinsic bulk PAS properties of HfO₂



As-deposited vs annealing (PVD, 50 nm thick layers)

- After annealing: Si characteristics reached more quickly, energy range governed by annihilation in HfO₂ narrowed. S ↑, W ↓.
- Defect concentration increases during annealing in HfO₂^{8,18,19}
- Positively charged defects at HfO₂/Si interface, created during annealing, result in a positive internal electrical field consistent with VEPFIT simulations



ALD vs PVD (50 nm thick layers)

- ALD before annealing
 - S ↑ and W ↓ compared to PVD layers
 - ALD curves very close to annealed PVD ones
- Higher defect concentration in ALD vs in PVD layers
- ALD after annealing
 - S ↑ and W ↓: [vacancy defects] increases
 - Slower evolution toward Si characteristics. Steady S and W in 1-5 keV energy range
- Negatively charged defects at HfO₂/Si interface, created during annealing, result in a negative internal electrical field consistent with VEPFIT simulations

Conclusion

- Slow positron beam DBS sensitive to the properties of HfO₂ layers down to a thickness of 50 nm on Si substrate.
- Void defect concentration in annealed layers higher than in the as deposited ones either by ALD or PVD process. As deposited ALD material revealed more defects concentration than the PVD probably due to the out-of-range thickness for the ALD process.
- Simulations of DBS parameters highlighted the role of a built-in electrical field related to charged defects at the HfO₂/Si interface
- Different behavior of ALD and PVD materials explained by different charged defects created during annealing
- However, quantitative analysis based on data reduction using complete DBS simulations still limited by the lack of the bulk parameters of the HfO₂ material → Thick layers of homogeneous properties required.
- To fulfill the nano-electronic specifications, coupling PAS with EELS-TEM analyses is mandatory.

Acknowledgements

This work was supported by the National Research Agency (ANR) through the French "Recherche Technologique de Base" Program. The experiments were performed in the frame of the joint development program with STMicroelectronics and the Nanocharacterisation platform (PFNC) at MINATEC.

We warmly thank, P. Hurlay, K. Cherkaoui, their team, the Tyndall National Institute (Ireland) for providing the 500 nm HfO₂ layer and A. Roule, H. Grampeix from LETI for providing ALD and PVD deposition.

References

- K. Shiraishi, et al., in: "Proc. of SISPAD", 306–313 (2006).
- K. Shiraishi, et al., *Thin Solid Films* **508**, 305–310 (2006).
- S. Guha and V. Narayanan, *Physical Review Letters* **98**, 196101 (2007).
- A. Kechichian, P. Barbois, and M. Gros-Jean, *ECS Transactions* **58**, 325–338 (2013).
- J. Robertson, O. Shariq, and A.A. Demkov, *Applied Physics Letters* **91**, 132912 (2007).
- G. Bersuker, et al., *Journal of Applied Physics* **100**, 094108 (2006).
- G. Bersuker, et al., *IEEE Transaction on Electron Devices* **57**, 2047–2056 (2010).
- A. Uedono, et al., *Japanese Journal of Applied Physics* **46**, 3214–3218 (2007).
- P. Calka, et al., *Nanotechnology* **24**, 085706 (2013).
- P.E. Lhuillier, et al., *Journal of Nuclear Materials* **416**, 13–17 (2011).
- P. Desgardin et al., *Applied Surface Science* **252**, 3231–3236 (2006)
- R. Krause-Rehberg, and H.S. Leipner, *Positron Annihilation in Semiconductors: Defect Studies*, Springer-Verlag, 1999.
- A. Uedono, et al., *Journal of Applied Physics* **100**, 034509 (2006).
- D.W. Gidley, et al., *Annual Review of Materials Research* **36**, 49–79 (2006).
- Z.W. Ma et al., *Thin Solid Films* **519**, 6349–6353 (2011).
- T. Belhabib, *TiN Behavior Under Irradiation: Interaction With Implantation Elements (He, I and Cs) and Defects Studies*. Master Thesis, University of Orleans, 2007.
- R. Kauppinen et al., *Journal of Physics: Condensed Matter* **9**, 10595 (1997).
- R.S. Brusa et al., *Radiation Physics and Chemistry* **76**, 189–194 (2007).
- R.S. Yu et al., *Nuclear Instr. and Methods in Phys. Res. Section B: Beam Inter. with Mat. and Atoms* **267**, 3097–3099 (2009)